PFC/JA-88-32

COMPARISON OF TWO ICCS CONDUCTORS AND FOR MHD APLLICATION *

Marston, P.G., Hale, J.R., Dawson, A.M.

August 22,1998

Plasma Fusion Center
Massachusetts Institute of Technology
Cambridge, M.4 02139

* Supported by the US Department of Energy, Pittsburgh Energy Technology Center under contact DE-AC22-84PC70512

COMPARISON OF TWO ICCS CONDUCTORS FOR MHD APPLICATION †

J. R. Hale, P.G. Marston and A.M. Dawson
Plasma Fusion Center
Massachusetts Institute of Technology
Cambridge, MA 02139

Abstract

Two subscale internally cooled, cabled superconductors have been examined as candidates for use in a retrofit MHD topping cycle magnet. One of these was a 3 × 3 × 3 cable in which all the strands were multifilamentary NbTi stabilized with copper. The other was a 3 × 3 × 3 cable in which two strands in each of the nine triplets was OFHC copper and one was multifilamentary NbTi. The overall copper-to-superconductor ratio for each of the two 27-strand cables was approximately the same. The two conductors were cowound onto a grooved mandrel in such a way that they could be tested alternately. Each sample was instrumented with a heater at the center of the conductor length, and with a pressure transducer, four pairs of voltage taps and one iron-doped gold/constantan thermocouple. Performance tests of the conductors were made at 6, 7 and 7.8 tesla background magnetic fields and at heater input energies ranging from 60 mJ/cm^3 to 1758 mJ/cm^3 of conductor. The results of these tests and their significance for MHD magnet design and economics are discussed.

Background and Conductor Design

One phase of a three-year program to develop and test an internally cooled, cabled superconductor (ICCS) for large-scale MHD magnets was a comparison test of two niobium-titanium (NbTi) subscale superconductors.[1-8] Type A was made of nine cabled triplets in which each strand contained filaments of superconductor along with copper stabilizer. For these strands the copper:superconductor ratio was 7:1. The Type B conductor contained triplets in which only one of the three strands contained superconductor in a copper:superconductor ratio of 1.35:1, while the other two strands were OFHC copper stabilizer. Type B conductor thus had an overall copper:superconductor ratio of 6.05:1. Both cables were wrapped with type 304 stainless steel foil, 0.0025 cm thick, and sheathed in type 304 stainless steel tubing. They were compacted to 35% void space (65% density). The finished dimensions were 0.41 cm od with an 0.051 cm sheath thickness. The test sample length was 4.6 m. Table I lists conductor parameters.

Table I
Characteristics of Superconductor Strands
for Conductor Types A and B

Characteristic	Type A	Type B
strand diameter	0.051 cm	0.051 cm
critical field	12.2 T	12.2 T
Cu:SC ratio	7:1	1.35:1
T_c at 6 T	6.4 K	6.4 K
T_c at 7 T	6.1 K	6.1 K
T_c at 8 T	5.6 K	5.6 K
I_c at 6 T	783 A	1215 A
I_c at 7 T	621 A	990 A
I_c at 8 T	459 A	675 A

†Supported in part by US Department of Energy, Pittsburgh Energy Technology Center under contract DE-AC22-84PC70512

Manuscript received August 22, 1988

The goal of the test program was to determine whether the Type B conductor was similar in stability, quench propagation, and pressure dynamics performance to the former, conventional design. If it were, it would offer a potential significant savings in manufacturing cost for a full-scale conductor.

Experiment Design

The two samples were cowound into a single-layer bifilar coil which is shown schematically in Fig. 1 and in a photograph in Fig. 2. The coil support mandrel is a 4.4" dia., 10" long grooved G-10 cylinder. The samples were connected electrically in series and so carried the same transport current at all times. However, only one sample at a time was subjected to an energy perturbation. The energy perturbation, designed to simulate frictional heating of the sheath, the principal potential source of heating in an MHD magnet, was administered through a heater soldered directly to the conductor sheath.

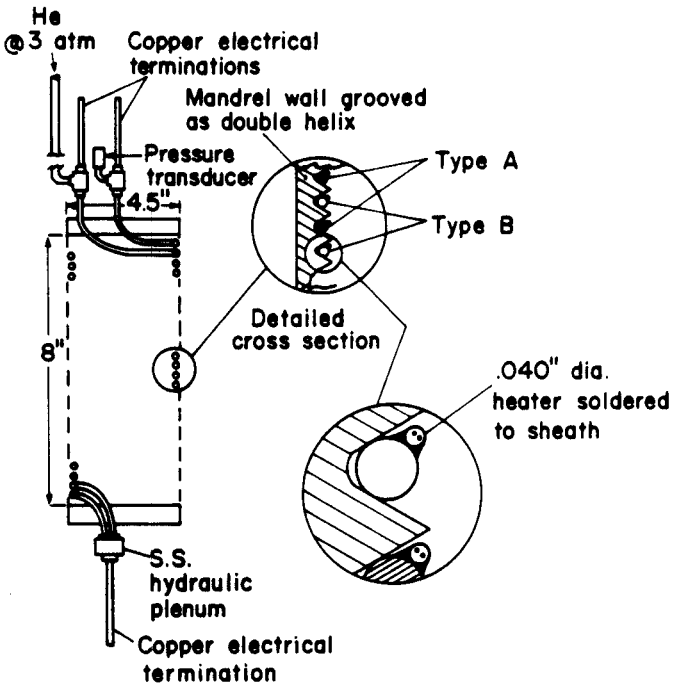

Figure 1 Schematic Illustration of Test Coil

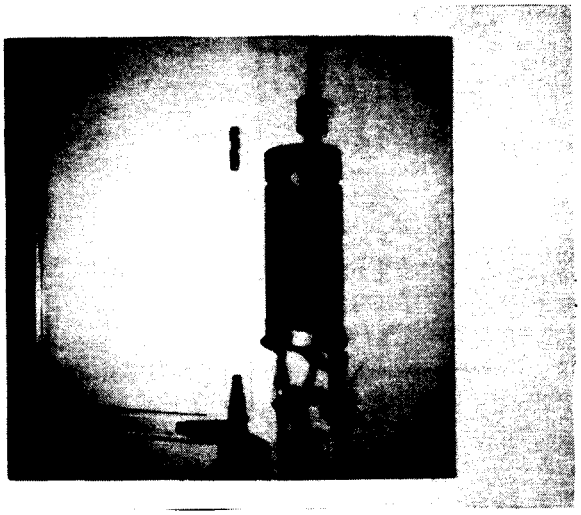

Figure 2 Photograph of Test Coil

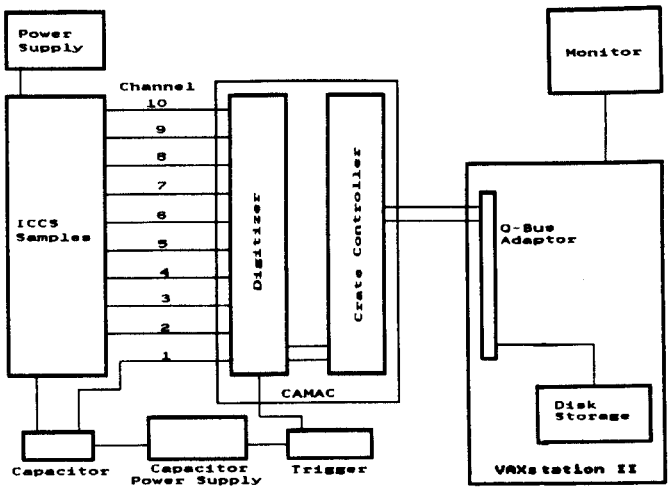

Figure 3 Schematic Illustration of Data Acquisition System

Data Collection and Test Procedure

Figure 3 is a schematic diagram of the data acquisition system. Ten analog signals, listed in Table II, were monitored. These were connected to the inputs of a LeCroy model 8212A 32-channel digitizer. The entire sequence of digitizing and storing the ten channels of data on Winchester disk was handled by the MIT MDS Software package.† Nine data channels were displayed on a video monitor a few seconds after each digitize/store sequence. Each experimental run was organized by shot number and each shot was initiated manually by discharging the capacitor into the heater. Simultaneously, the data acquisition system began to convert and store the ten signals, and continued for two seconds, with a time resolution of 500 μs, yielding 4096 data points per channel for each shot.

Table II
Data Monitored by Channel

Channel	Parameter Monitored
1	Current through pulse heater
2	Voltage across heater terminals
3	Thermocouple voltage
4	Potential difference on surface of sheath between the ends of the heated length
5	Potential difference across one turn, ~ one turn above heated length
6	Potential difference across one turn, ~ one turn below heated length
7	Total potential difference between ends of test sample
8	Transport current in sample
9	Pressure inside sheath
10	Total potential difference between ends of the unperturbed sample

† ©1986 Massachusetts Institute of Technology

Testing of each sample was carried out at three levels of background field: 6 T, 7 T, and 7.8 T, provided by the 6B magnet at the Francis Bitter National Magnet Laboratory. Once the background field was set, the following looping sequence was used:

1. Transport current set to desired value.
2. Capacitor charged to desired voltage, initial choices based on analysis of expected performance, later choices on results of prior shots.
3. Capacitor discharged into heater by manual trigger, simultaneously triggering data acquisition system.
4. Sample voltage monitored on oscilloscope – if voltage rise is rapid, indicating propagating normal zone, current supply interrupted to avoid sample damage.
5. Return to step 1, if more data is needed at preset field level; otherwise change background field level and return to step 1.

The critical current of Type A conductor was measured at each of the three levels of background field. Since the current capacity of Type A was lower than that of Type B, and the two were in series, it was not possible to measure the critical current of Type B directly.

Results

Early in the project two worst-case scenarios for conductor performance had been analysed. Because the measured critical current of Sample A exceeded the value claimed by the manufacturer, these calculations were repeated to provide a more realistic basis by which to evaluate conductor experimental performance. Both scenarios had the common characteristic that nonrecovery from a heat pulse is inevitable if the temperature of the helium is driven above the current-sharing temperature. The difference between the two scenarios is that in case I the initial perturbation is a small fraction of that required to raise the helium to this temperature, with the balance coming from joule heating, while in case II the initial perturbation supplies all the input energy required to bring the helium to this temperature.

The input to the stability analysis program, in addition to the values in Table I, included an initial pressure of 3 atm, an initial temperature of 4.2 K and an energy perturbation of a single half-sinusoidal pulse 20 ms in duration. In case I the perturbation was applied to the full length of the conductor. Heat flows by conduction directly from the heated sheath to the strands such that the temperature distribution at time Δt_I following the perturbation is nearly identical to that if the same energy pulse were applied directly to the strands throughout the entire length of conductor. In case II the heat was transferred from the sheath such that at time Δt_{II} following the perturbation, the temperatures of the sheath, the helium and the strands are the same. Δt_I and Δt_{II} are estimates at best, and range from 1 to 20 ms. For conductor Type A the energy margin for worst case II is for the most part larger than for worst case I in which current-sharing occurs.

The Type B conductor calculations were complicated by the fact that the existing stability program has no means for 'hybriding' the strands in a cable. Therefore, the copper strands were considered to be both electrically and thermally innocuous, leaving only the very low copper-to-superconductor ratio of the nine superconducting strands which led to high joule heating for case I. For case II, however, all 27 strands contributed enthalpy and raised the energy margin to much greater values than case I.

The degree to which these calculated scenarios are representative of the physical arrangement of the constituent materials, and of the physical processes that occurred during the experimental testing was expected to be modest at best. For example, in calculating Worst Case I, the perturbation was applied to the strands as a 10 ms inductive pulse over the whole length of the sample. The intent for the experiment, on the other hand, was to apply the perturbation to 30 cm of the $\sim$ 4.6 m samples as a 10 ms heater current pulse to a heater soldered to the sheath. As thermocouple data showed later, however, it is likely that although the current pulse was 10 ms in duration, the actual pulse of heat energy at *the sheath surface* was more nearly 500 ms in duration; evidently, the ceramic insulation within the heater was much more of a barrier than expected.

The following series of data from Type A conductor shown in Figs. 4-6 also indicates that actual behavior is more complex than that assumed in the computer model. The top trace in each plot is the thermocouple output, referenced to 0 K.† The middle trace is the resistance of the heated length of conductor, and the bottom trace is the total resistance of the sample. Superimposed on all three traces is the trace of transport current‡, with the scale indicated on the right side axis.

Figures 4 and 5 show a pair of sequential shots, one of which led to a propagating normal zone (#81), and one that did not (#80). In #80, current-sharing commences at about 200 ms, but collapses after lasting for about 350 ms. A similar situation can be seen in the trace of shot #110 (Figure 6), although current-sharing in that case lasted longer. These traces show evidence that at least some of the strands are heated by contact with the sheath to a temperature above that of the interstitial helium, which is also being heated by contact with the sheath. But the source of heat — the sheath — reaches a temperature lower than the current-sharing temperature, T_{cs}, before the helium temperature rises to T_{cs}, and therefore, the helium can continue to serve as a heat sink for the heated strands. In these two shots, the strands were able to cool to less than T_{cs}, despite the joule heating addition to their energy burden.

Shot #81 shows a case in which the strands, once current-sharing set in, were not cooled to less than T_{cs} before the interstitial helium's temperature was raised to T_{cs} by contact with sheath and the warming strands.

In order to measure the speed with which a normal zone would grow, voltage taps were attached to the sheath approximately three turns (24 inches) beyond the heated length in both directions. From limited data, the speed of propagation of the T_{cs} regime was calculated to be approximately 1.3 m/s. Additional data with voltage taps repositioned to be closer to the ends of the heated length would make it possible to verify this value.

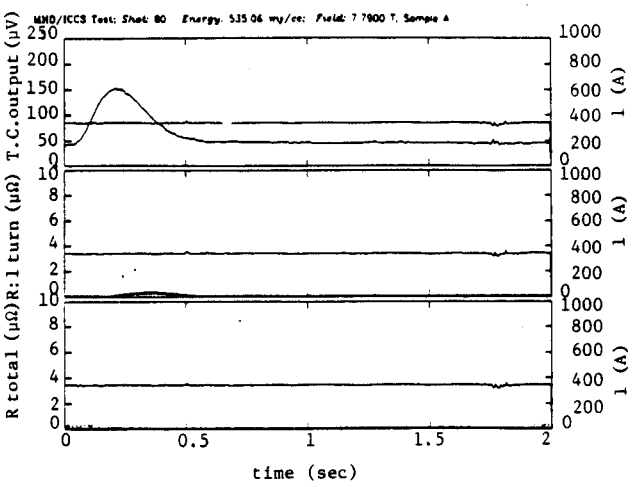

Figure 4 Example of a Shot Showing Initiation and Collapse of a Normal Zone

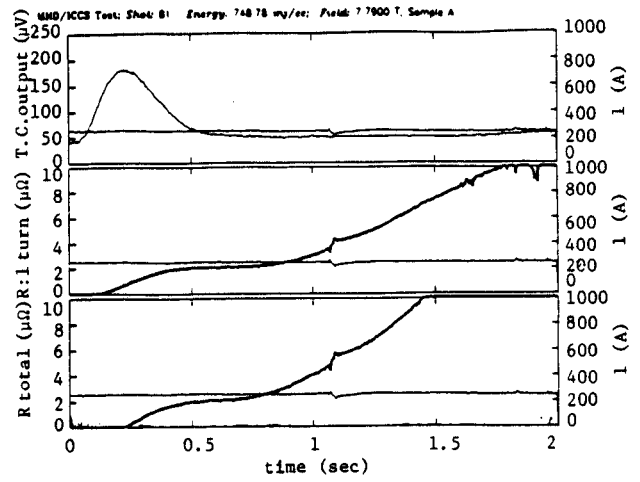

Figure 5 The Subsequent Shot in Which a Propagating Normal Zone Develops

† 40 μV = 4 K, 150 μV = 11.4 K, 250 μV = 17.3 K.

‡ The decay in current apparent whenever current-sharing is underway is due to the fact that the power supply acts as a constant voltage source rather than as a constant current source.

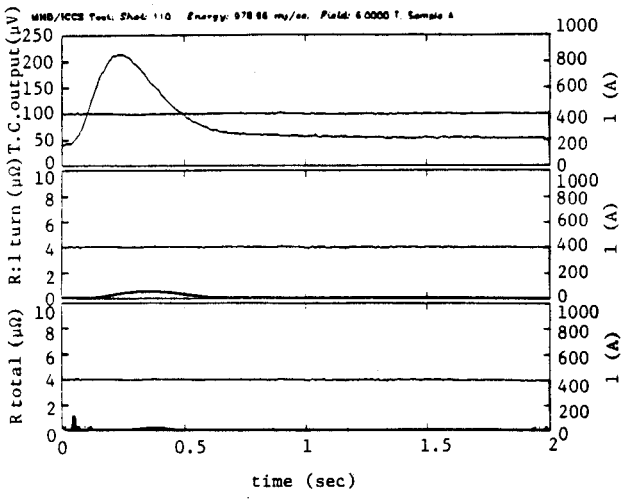

Figure 6 An Example of a Long Current-Sharing Period with No Propagating Normal Zone

Conclusions

Inasmuch as the effective duration of the energy pulse was greater than had been intended, no conclusions can be drawn regarding the comparative stability of these two conductors against short duration (1—10 millisecond) perturbations. The conclusions regarding their response to longer duration (a few hundred millisecond) heat inputs applied to the surface of the sheath are:

1) If operated at equivalent I/Ic, these two conductors will behave comparably with respect to their response to so-called 'long' duration heat perturbations at the sheath surface.

2) There is good thermal heat-sink action provided by the interstitial helium, enough so that the bulk of the energy needed to raise the temperature of the strands to T_{cs} comes from the initial source of the perturbation.

3) Although the thermal contact between the strands and the sheath may be intermittent along a given conductor length, it is adequate to enable at least some of the strands to be heated by conduction from the inner surface of the sheath. This suggests that the electrical contact is also moderately good, although not necessarily equally good to all strands in any given length interval.

The general conclusion to be drawn from the tests is that it is reasonable to assume that the lower cost two-in-one triplet cable configuration will be perfectly satisfactory for large-scale NbTi internally cooled, cabled superconductors. Such performance must, of course, be verified at full scale.

References

[1] Design Requirements Definition Report for ICCS for Large Scale MHD Magnets, Plasma Fusion Center, MIT, Cambridge, MA, November 1985.

[2] Analysis Report, Develop and Test an Internally Cooled, Cable Superconductor (ICCS) for Large-Scale MHD Magnets, MIT, January 1986, DOE/PC-70512-5.

[3] Develop and Test an Internally Cooled, Cabled Superconductor for Large-Scale MHD Magnets: Test Plan, August 1986, Revised May 1987, DOE/PC-70512-5.

[4] Develop and Test an Internally Cooled, Cabled Superconductor for Large-Scale MHD Magnets: Semiannual Progress Report, January 1 to June 30, 1987, DOE/PC-70512-10, Sept. 1987.

[5] C.J. Heyne, D.T. Hackworth, S.K. Singh, Y.L. Young, Westinghouse Design of a Forced Flow Nb_3Sn Test Coil for the Large Coil Program, and references therein, Eighth Symposium On Engineering Problems in Fusion Research, pp 1148-1153, 1979.

[6] P.A. Materna, Design Considerations of Forced-flow Superconductors in Toroidal Field Coils, Tenth Symposium on Engineering Problems in Fusion Research, pp 1741-1746, 1983.

[8] L. Dresner, D.T. Fehling, M.S. Lubell, J.W. Lue, J.N. Luton, J. McManamy, C.T. Wilson, R.E. Wintenberg, Stability Tests of the Westinghouse Coil in the IFSMTF, Tenth International Conference on Magnet Technology, Sep. 1987, to be published in *IEEE Trans. Mag.*, March 1988.